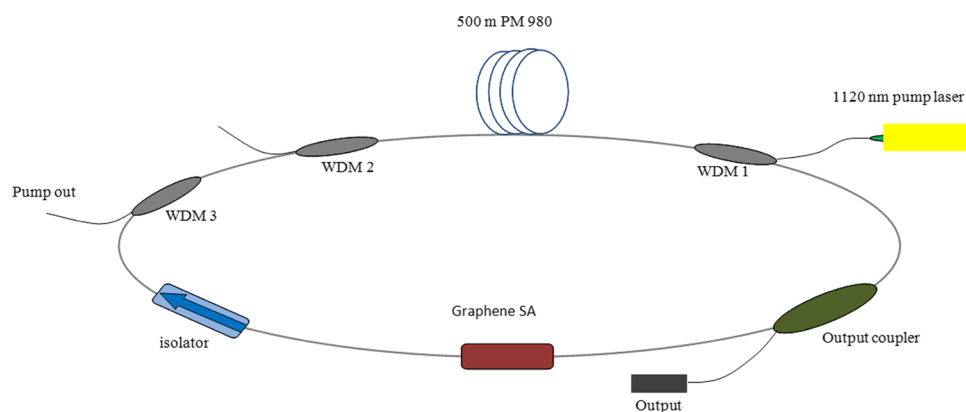


Linearly Polarized 1180-nm Raman Fiber Laser Mode Locked by Graphene

Volume 4, Number 5, October 2012

Lei Zhang
Gaozhong Wang
Jinmeng Hu
Jianhua Wang
Jintai Fan
Jun Wang
Yan Feng



DOI: 10.1109/JPHOT.2012.2218231
1943-0655/\$31.00 ©2012 IEEE

Linearly Polarized 1180-nm Raman Fiber Laser Mode Locked by Graphene

Lei Zhang,^{1,2} Gaozhong Wang,^{2,3} Jinmeng Hu,^{1,2} Jianhua Wang,¹
Jintai Fan,³ Jun Wang,³ and Yan Feng¹

¹Shanghai Key Laboratory of Solid State Laser and Application and Shanghai Institute of Optics and Fine Mechanics, Chinese Academy of Sciences, Shanghai 201800, China

²Graduate University of the Chinese Academy of Sciences, Beijing 100049, China

³Key Laboratory of Materials for High Power Laser, Shanghai Institute of Optics and Fine Mechanics, Chinese Academy of Sciences, Shanghai 201800, China

DOI: 10.1109/JPHOT.2012.2218231
1943-0655/\$31.00 ©2012 IEEE

Manuscript received August 9, 2012; revised September 6, 2012; accepted September 6, 2012. Date of current version September 20, 2012. This work was supported in part by the 100-Talent Program of Chinese Academy of Sciences and in part by the National Natural Science Foundation of China under Grant 61178007. Corresponding author: Y. Feng (e-mail: yanfeng@siom.ac.cn).

Abstract: In this paper, we demonstrate a linearly polarized 1180-nm passively mode-locked Raman fiber laser using graphene-based saturable absorber (SA). The pump source is a linearly polarized ytterbium-doped fiber laser at 1120 nm. Stable nanosecond mode-locked pulses with a repetition rate of 0.4 MHz are generated. The combination of Raman technology and the graphene-based ultrawide bandwidth SA offer a prospect of real wavelength-versatile mode-locked laser source. The mode-locked laser operating at 1180 nm is suitable for frequency doubling to yellow light after amplification.

Index Terms: Mode-locked lasers, fiber nonlinear optics, optical properties of photonic materials.

1. Introduction

Graphene is a 2-D honeycomb lattice of carbon atoms that has outstanding electrical and optical properties [1], [2]. Graphene is used as a saturable absorber (SA) for mode-locked lasers because of its ultrabroadband saturable absorption and ultrafast recovery time. Its ultrabroadband saturable absorption facilitates the mode locking of lasers at different wavelengths, which has been demonstrated at 1.5 μm [3]–[6] and 1 μm [7] with different gain media. However, these rare-earth-doped laser gain media have a limited operating wavelength range, and the advantage of the ultrabroadband saturable absorption is not fully utilized.

Raman fiber lasers have the same wavelength flexibility as graphene because Raman gain is available at arbitrary wavelengths across the transparency window of optical fibers (300 nm to 2300 nm for silica fiber) with the right pump source [8]. It was originally developed for telecommunications [9] and was later utilized for generating high-powered lasers at special wavelengths for specific applications [10]–[12]. The mode locking of Raman fiber lasers has been demonstrated with dissipative four-wave mixing [13], nonlinear loop mirrors [14], nonlinear polarization evolution (NPE) [15], semiconductor SA mirror (SESAM) [16], and nanotubes [17].

In this paper, we demonstrate a mode-locked Raman fiber laser with graphene as SA, which combines the shared advantages of graphene and stimulated Raman scattering in spectral versatility. The laser is pumped with a linearly polarized Yb-doped fiber laser at 1120 nm and operates at

1180 nm with a repetition rate of 0.4 MHz, a typical pulse duration of 200 ns, and a maximum pulse energy of 165 nJ. The laser source is suitable for frequency doubling to yellow light after amplification, which has wide applications in metrology, remote sensing, and medicine. Efficient amplification can be achieved with a Raman fiber amplifier [12], [18].

Recently, Castellani *et al.* [19] reported graphene mode-locked Raman fiber laser at 1.5 μm . In their work, the laser usually operated at higher harmonics of the cavity repetition rate, which made the pulse energy very low (~ 10 nJ). The results in this paper are significantly different, with the mode locking consistently at the fundamental repetition rate. In addition, our laser setup features all-polarization maintaining (PM), which not only facilitates the generation of an environmentally stable linearly polarized output but also excludes the contribution of NPE in pulse forming.

2. Preparation of the Graphene SA

We followed the procedure used in [20] and [21] in preparing the graphene dispersions. The experimental and theoretical analyses reveal that the surface energies of the selected solvents, namely, *N,N*-dimethylformamide (DMF), *N*-methyl-2-pyrrolidone (NMP), *N,N*-dimethylacetamide (DMA), and γ -butyrolactone (GBL), match very well with that of graphite (~ 70 mJ m^{-2} to 80 mJ m^{-2}), resulting in a minimal energy cost for overcoming the van der Waals forces between graphene sheets, hence the effective exfoliation into single or a few layers of graphene [22]. Graphite from Sigma-Aldrich was used. The dispersions of graphene were prepared in DMF at an initial concentration of 5.0 mg/mL. In general, the initial dispersions were produced by sonication for 24 h using a low-power ultrasonic bath (200 W). The dispersions were then left to stand at room temperature for 24 h. All dispersions were subsequently centrifuged at 1500 r/min for 90 min to remove any large aggregates. High-quality dispersions were obtained by collecting the top part of the centrifuged samples. The dispersions were stable against sedimentation and displayed no further aggregation for a period of weeks.

The state of the dispersed graphene was observed using transmission electron microscopy (TEM). The TEM samples were prepared by dropping a few milliliters of dispersion onto copper holey carbon grids. Fig. 1(a) and (b) shows typical bright-field TEM images of the graphene flakes, which imply the presence of a monolayer and few-layer graphene in the dispersions.

The graphene was transferred onto the end face of a fiber pigtail via optically driven deposition [23]. The optical source is a single-mode laser diode at 976 nm. Fig. 1(c) shows the image of the fiber end face after 10-min optical deposition under an optical power of 30 mW, where the well-distributed graphene is deposited onto the fiber core. If the output power is increased to 60 mW and the deposition time is shortened to 5 min, a clear ring-structured spread of graphene is observed around the fiber core, as shown in Fig. 1(d), which is unsuitable for SAs. The SAs used in the experiments are optically deposited for 10 min under an optical power of 30 mW [shown in Fig. 1(c)]. The complete SA unit is produced by joining the graphene-deposited fiber pigtail and a clean fiber pigtail with a mating sleeve.

The nonlinear optical absorption of the graphene-based SA was investigated with a mode-locked fiber laser at 1053 nm as a probe laser. Fig. 2(a) shows the measured transmission as a function of the launched fluence. The saturable and nonsaturable losses were 24% and 33%, respectively. The saturation fluence was determined to be about 1300 $\mu\text{J}/\text{cm}^2$, where the saturable loss reduced by 37%. The high saturable loss indicates that multiple single or few-layer graphene flakes were present on the light path. This is not surprising because the fiber end is likely to be stacked up with many graphene flakes during optical deposition, which can be seen in Fig. 1(c). The relatively high nonsaturable loss is due to the decreased coupling efficiency between the fiber pigtails because of the light scattering by the thick graphene flakes on the fiber end.

3. Experimental Setup of the Mode-Locked Raman Fiber Laser

The experimental setup of the Raman fiber laser is shown in Fig. 2(b). Five hundred meters of PM single-mode fiber (PM980) is used as the Raman gain medium, which has an estimated Raman

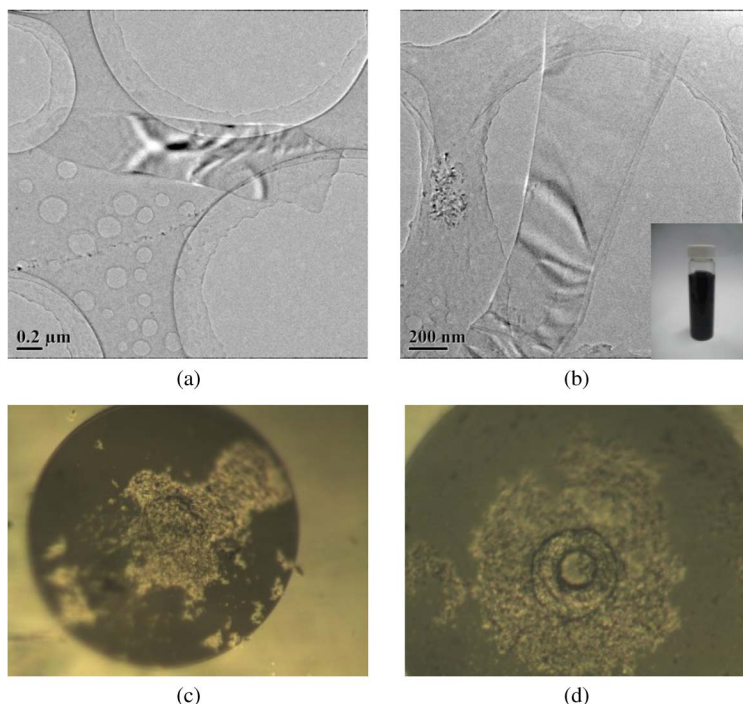


Fig. 1. (a) and (b) *TEM images* of graphene flakes in the dispersions. Fiber end-face after graphene deposition under the following conditions: (c) 30 mW, 10 min; (d) 60 mW, 5 min.

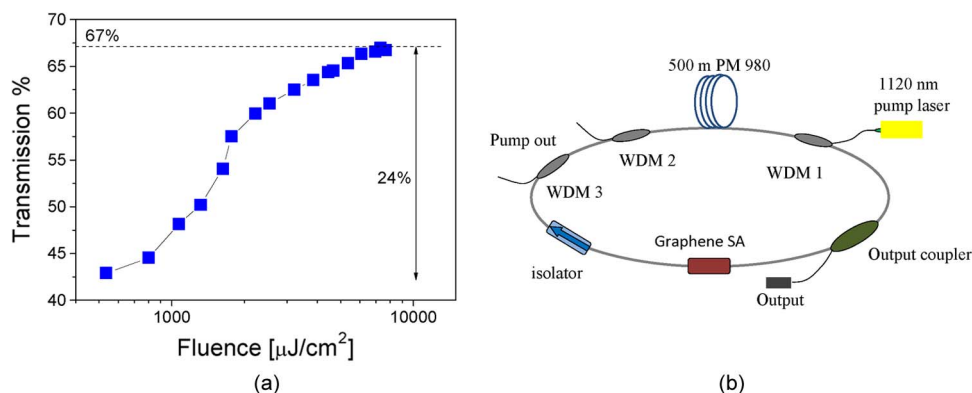


Fig. 2. (a) Transmission of the graphene-based SA unit versus launched fluence of a short pulse laser at 1053 nm. (b) Experimental setup of the graphene mode-locked Raman fiber laser.

gain coefficient of $1.8 \text{ W}^{-1} \text{ km}^{-1}$ at 1120 nm. The net cavity dispersion value is 8.13 ps^2 . The fiber laser is backward pumped by a linearly polarized 10-W Yb-doped 1120-nm fiber laser with a polarization extinction ratio (PER) of 20 dB through a PM 1120/1180-nm wavelength division multiplexer (WDM). Two 1120/1180-nm WDMs are attached at the other end of the gain fiber as residual pump extractors to prevent possible damage to the optical components. An optical isolator is inserted into the cavity to ensure unidirectional light propagation. The graphene SA is integrated after the isolator, followed by a 7% output fiber coupler. To eliminate environmental sensitivity and the possibility of mode locking by NPE, which is often associated with a non-PM fiber laser, an all-PM configuration is constructed. Consequently, we can make sure that the graphene SA is responsible for initiating and sustaining the pulsed operation.

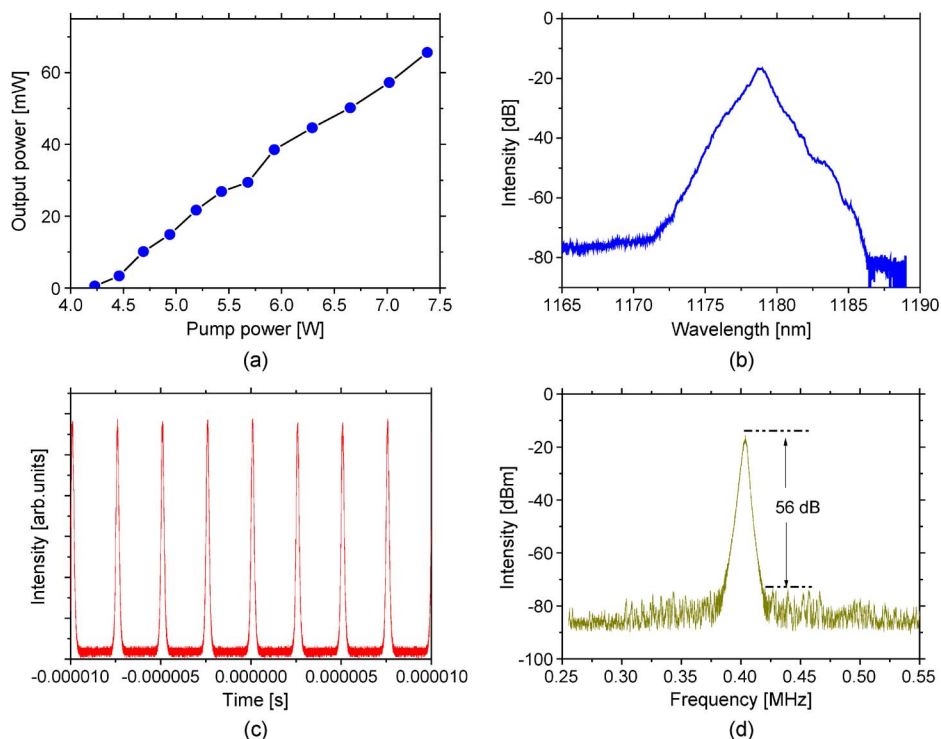


Fig. 3. (a) Output power of the laser as a function of pump power. (b) The spectrum of the Raman fiber laser at a pump power of 5 W. (c) Mode-locked pulse trains with a repetition rate of 0.4 MHz. (d) RF spectrum of the mode-locked laser output.

4. Laser Results and Discussions

Self-starting mode-locked operation was obtained when the pump power increased to above the threshold from 4.3 W to 7.4 W without any preceding Q-switching state, which is very different from rare-earth-doped mode-locked fiber laser. Further increase of the pump power caused the mode-locked operation to cease. However, the mode-locked operation recovered when we decreased the pump power. The essentially different startup process is determined by the ultrafast gain dynamics in Raman fiber laser (fs) and the slow gain relaxation dynamics in rare-earth-doped medium (100 μ s to 10 ms) [15], [16]. The slow gain relaxation dynamics of rare-earth-doped medium favors efficient energy storage in the laser cavity, which usually facilitates the Q-switching instability. By contrast, in mode-locked Raman fiber laser, forming macro Q-switched pulses that cover multiple roundtrip times is not possible. Therefore, the mode-locked pulse train develops directly from continuous-wave noise radiation. In graphene or nanotube mode-locked fiber lasers, the often-observed damage of SA is due to giant Q-switched pulses; hence, the different startup process in mode-locked Raman fiber laser is rather advantageous. We observed short lifetime of the graphene SA in our Yb fiber laser experiments, and similar state could be found in [24], whereas the graphene SA in the mode-locked Raman fiber laser experiments remained in good condition throughout the experiments for weeks.

Fig. 3(a) shows the output power of the laser versus the pump power. The maximum output power was 60 mW, with a PER of 12 dB, which is limited by the PER of the output fiber coupler (13 dB). The optical efficiency is low because of the high intracavity loss and the low Raman gain at a pump power of several watts. The output spectrum of the Raman fiber laser, measured at a pump power of 5 W, is shown in Fig. 3(b). The peak wavelength is at 1180 nm, and the spectral bandwidth (FWHM) was 0.9 nm, measured by an optical spectral analyzer with a resolution of 0.02 nm. Fig. 3(c) shows the Raman mode-locking pulse trains with a repetition rate of 0.4 MHz, which matches the optical length of the cavity. The pulse duration is typically as long

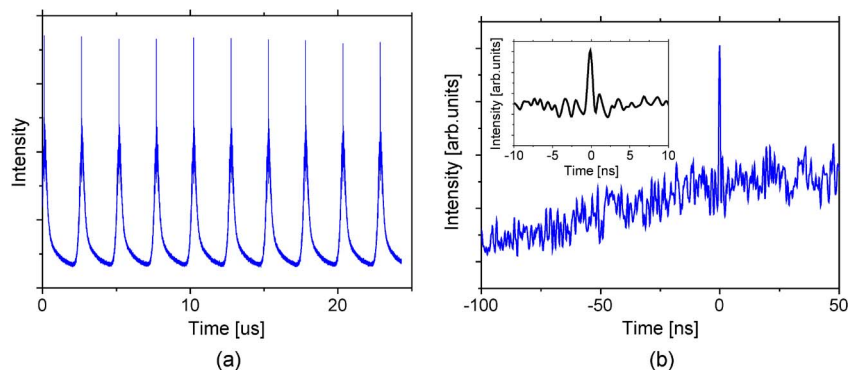


Fig. 4. (a) pulse trains with a sharp spike on the top. (b) Zoomed-in view of the sharp spike. Inset is a further zoomed-in image of the sharp peak, which shows a resolution-limited width of 700 ps.

as 200 ns, and the pulse duration is almost constant with the change of output power. Fig. 3(d) shows a radio frequency (RF) spectrum measured around the fundamental repetition rate. A 56-dB peak-to-background ratio was observed, which indicates good mode-locking stability and low pulse timing jitter.

The broad pulses in Raman fiber laser can be viewed as the counterpart of Q-switched pulses in rare-earth-doped fiber laser, although the pulsewidth with respect to the cavity roundtrip time is very different. In Raman fiber laser, the only energy “storage” mechanism is light propagation through the fiber cavity; therefore, the “Q-switched” pulses have a width that is shorter than one roundtrip time and a repetition rate that is equal to c/nL , where c is the light speed, and nL is total cavity optical length. The long pulse generation can be reproduced with a rate equation model, which will be presented in a future dedicated publication.

It is interesting to note that, occasionally, the 200-ns-long pulses has a sharp peak with a duration of resolution-limited 700 ps on the top, as shown in Fig. 4(a). However, these type of pulses are not stable and does not persist for long time. Similar phenomenon had been observed in mode-locked Raman fiber lasers with semiconductor SA and NPE [15], [16]. Since the laser cavity is formed with normal dispersion components, the short pulse on top of the long pulse is possibly the result of dissipative soliton mode locking [25], [26]. The necessary spectral filtering is provided by the three 1120/1180-nm WDMs and one output coupler, which collectively have a bandwidth of ~ 10 nm. However, the typical spectrum with sharp edges for dissipative soliton mode locking was not observed because the laser power of the short pulses was only a small fraction of the power of the long pulses.

In our experiments, the laser always works at the fundamental repetition rate, which is very different from the observation in reference [19], wherein the laser usually operates at the higher harmonics of the cavity repetition rate. This difference with reference [19] is caused by the use of a single few-layer graphene film as SA in their work, which has very weak absorption. Harmonic mode locking is likely to occur if the SA has weak absorption. However, in this paper, the modulation depth was as high as 24%. The high modulation depth of the graphene SA plays a key role in suppressing the noise pulse and achieving single-pulse mode locking.

The formation of the long pulse train is interesting in physics. However, pure short pulses are usually more interesting in practice. Our next step is to reduce and eventually remove the long pulse component, which will require further investigation of the pulse formation mechanism and the necessary fine tuning of the Raman fiber laser setup. In the current experiments, the laser operated in a normal dispersion regime. The recent development in all-normal-dispersion mode locking [26] provides some potential solutions to achieving stable and ultrashort pulse mode-locked Raman fiber lasers, in which spectral filtering [27] is particularly interesting because it can be applied simultaneously to demonstrate the tunability of Raman fiber lasers.

5. Summary

In summary, we report the use of graphene for mode-locking Raman fiber laser, which combines the shared advantage of graphene and stimulated Raman scattering in spectral versatility. The laser is pumped with an Yb fiber laser at 1120 nm and operated at 1180 nm with a repetition rate of 0.4 MHz and pulsewidth typically 200 ns long. Pulses with an unstable sharp spike on the top with a duration of resolution-limited 700 ps is also observed. The combination of Raman gain and the graphene-based ultrabroadband SA provides a potential solution for obtaining ultrafast laser at virtually any wavelength of interest. Our next step is to further investigate the forming mechanism of both the short and long pulses, and then improve the laser performance by removing the long pulses.

References

- [1] A. K. Geim and K. S. Novoselov, "The rise of graphene," *Nat. Mater.*, vol. 6, no. 3, pp. 183–191, Mar. 2007.
- [2] F. Bonaccorso, Z. Sun, T. Hasan, and A. C. Ferrari, "Graphene photonics and optoelectronics," *Nat. Photon.*, vol. 4, no. 9, pp. 611–622, Sep. 2010.
- [3] T. Hasan, Z. Sun, F. Wang, F. Bonaccorso, P. H. Tan, A. G. Rozhin, and A. C. Ferrari, "Nanotube-polymer composites for ultrafast photonics," *Adv. Mater.*, vol. 21, no. 38/39, pp. 3874–3899, Oct. 2009.
- [4] Q. Bao, H. Zhang, Y. Wang, Z. Ni, Y. Yan, Z. X. Shen, K. P. Loh, and D. Y. Tang, "Atomic-layer graphene as a saturable absorber for ultrafast pulsed lasers," *Adv. Funct. Mater.*, vol. 19, no. 19, pp. 3077–3083, Oct. 2009.
- [5] D. Popa, Z. Sun, F. Torrisi, T. Hasan, F. Wang, and A. C. Ferrari, "Sub 200 fs pulse generation from a graphene mode-locked fiber laser," *Appl. Phys. Lett.*, vol. 97, no. 20, pp. 203106-1–203106-3, Nov. 2010.
- [6] Z. Sun, T. Hasan, F. Torrisi, D. Popa, G. Privitera, F. Wang, F. Bonaccorso, D. M. Basko, and A. C. Ferrari, "Graphene mode-locked ultrafast laser," *ACS Nano*, vol. 4, no. 2, pp. 803–810, Jan. 2010.
- [7] Z. Luo, M. Zhou, J. Weng, G. Huang, H. Xu, C. Ye, and Z. Cai, "Graphene-based passively Q-switched dual-wavelength erbium-doped fiber laser," *Opt. Lett.*, vol. 35, no. 21, pp. 3709–3711, Nov. 2010.
- [8] G. P. Agrawal, *Nonlinear Fiber Optics*. New York: Academic, 2007.
- [9] J. Bromage, "Raman amplification for fiber communications systems," *J. Lightwave Technol.*, vol. 22, no. 1, pp. 79–93, Jan. 2004.
- [10] J. W. Nicholson, M. F. Yan, P. Wisk, J. Fleming, F. DiMarcello, E. Monberg, T. Taunay, C. Headley, and D. J. DiGiovanni, "Raman fiber laser with 81 W output power at 1480 nm," *Opt. Lett.*, vol. 35, no. 18, pp. 3069–3071, Sep. 2010.
- [11] Y. Feng, L. R. Taylor, and D. B. Calia, "150 W highly-efficient Raman fiber laser," *Opt. Exp.*, vol. 17, no. 26, pp. 23 678–23 683, Dec. 2009.
- [12] Y. Feng, L. R. Taylor, and D. B. Calia, "25 W Raman-fiber-amplifier-based 589 nm laser for laser guide star," *Opt. Exp.*, vol. 17, no. 21, pp. 19 021–19 026, Oct. 2009.
- [13] J. Schroder, S. Coen, F. Vanholsbeeck, and T. Sylvestre, "Passively mode-locked Raman fiber laser with 100 GHz repetition rate," *Opt. Lett.*, vol. 31, no. 23, pp. 3489–3491, Dec. 2006.
- [14] D. A. Chestnut and J. R. Taylor, "Wavelength-versatile subpicosecond pulsed lasers using Raman gain in figure-of-eight fiber geometries," *Opt. Lett.*, vol. 30, no. 22, pp. 2982–2984, Nov. 2005.
- [15] A. Chamorovskiy, A. Rantamäki, A. Sirbu, A. Mereuta, E. Kapon, and O. G. Okhotnikov, "1.38- μm mode-locked Raman fiber laser pumped by semiconductor disk laser," *Opt. Exp.*, vol. 18, no. 23, pp. 23 872–23 877, Nov. 2010.
- [16] A. Chamorovskiy, J. Rautiainen, J. Lyytikäinen, S. Ranta, M. Tavast, A. Sirbu, E. Kapon, and O. G. Okhotnikov, "Raman fiber laser pumped by a semiconductor disk laser and mode locked by a semiconductor saturable absorber mirror," *Opt. Lett.*, vol. 35, no. 20, pp. 3529–3531, Oct. 2010.
- [17] C. E. S. Castellani, E. J. R. Kelleher, J. C. Travers, D. Popa, T. Hasan, Z. Sun, E. Flahaut, A. C. Ferrari, S. V. Popov, and J. R. Taylor, "Ultrafast Raman laser mode-locked by nanotubes," *Opt. Lett.*, vol. 36, no. 20, pp. 3996–3998, Oct. 2011.
- [18] L. Taylor, Y. Feng, D. Bonaccini Calia, and W. Hackenberg, "Multi-watt 589-nm Na D2-line generation via frequency doubling of a Raman fiber amplifier: A source for LGS-assisted AO," in *Proc. SPIE*, vol. 6272, *Advances in Adaptive Optics II*, 2006, p. 627 249.
- [19] C. E. S. Castellani, E. J. R. Kelleher, Z. Luo, K. Wu, C. Ouyang, P. P. Shum, Z. Shen, S. V. Popov, and J. R. Taylor, "Harmonic and single pulse operation of a Raman laser using graphene," *Laser Phys. Lett.*, vol. 9, no. 3, pp. 223–228, Mar. 2012.
- [20] Y. Hernandez, V. Nicolosi, M. Lotya, F. M. Blighe, Z. Sun, S. De, I. T. McGovern, B. Holland, M. Byrne, Y. K. Gun'Ko, J. J. Boland, P. Niraj, G. Duesberg, S. Krishnamurthy, R. Goodhue, J. Hutchison, V. Scardaci, A. C. Ferrari, and J. N. Coleman, "High-yield production of graphene by liquid-phase exfoliation of graphite," *Nat. Nanotechnol.*, vol. 3, no. 9, pp. 563–568, Sep. 2008.
- [21] J. Wang, Y. Hernandez, M. Lotya, J. N. Coleman, and W. J. Blau, "Broadband nonlinear optical response of graphene dispersions," *Adv. Mater.*, vol. 21, no. 23, pp. 2430–2435, Jun. 2009.
- [22] J. N. Coleman, "Liquid-phase exfoliation of nanotubes and graphene," *Adv. Funct. Mater.*, vol. 19, no. 23, pp. 3680–3695, Dec. 2009.
- [23] J. W. Nicholson, R. S. Windeler, and D. J. DiGiovanni, "Optically driven deposition of single-walled carbon-nanotube saturable absorbers on optical fiber end-faces," *Opt. Exp.*, vol. 15, no. 15, pp. 9176–9183, Jul. 2007.

- [24] K. Kieu and F. W. Wise, "All-fiber normal-dispersion femtosecond laser," *Opt. Exp.*, vol. 16, no. 15, pp. 11 453–11 458, Jul. 2008.
- [25] W. H. Renninger, A. Chong, and F. W. Wise, "Pulse shaping and evolution in normal-dispersion mode-locked fiber lasers," *IEEE J. Sel. Topics Quantum Electron.*, vol. 18, no. 1, pp. 389–398, Jan./Feb. 2012.
- [26] F. W. Wise, A. Chong, and W. H. Renninger, "High-energy femtosecond fiber lasers based on pulse propagation at normal dispersion," *Laser Photon. Rev.*, vol. 2, no. 1/2, pp. 58–73, Apr. 2008.
- [27] B. G. Bale, J. N. Kutz, A. Chong, W. H. Renninger, and F. W. Wise, "Spectral filtering for mode locking in the normal dispersive regime," *Opt. Lett.*, vol. 33, no. 9, pp. 941–943, May 2008.